



PLURIPOTENT STEM CELLS

Neurotrophin-3 contributes to benefits of human embryonic stem cell-derived cardiovascular progenitor cells against reperfused myocardial infarction

Wei Bi¹ | Jinxi Wang¹ | Yun Jiang¹ | Qiang Li¹  | Shihui Wang¹ |
Meilan Liu¹ | Qiao Liu¹ | Fang Li¹ | Christian Paul² | Yigang Wang² |
Huang-Tian Yang^{1,3,4} 

¹CAS Key Laboratory of Tissue Microenvironment and Tumor, Laboratory of Molecular Cardiology, Shanghai Jiao Tong University School of Medicine & Shanghai Institute of Nutrition and Health, University of Chinese Academy of Sciences (CAS), CAS, Shanghai, People's Republic of China

²Department of Pathology and Laboratory Medicine, College of Medicine, University of Cincinnati Medical Center, Cincinnati, Ohio

³Translational Medical Center for Stem Cell Therapy & Institute for Heart Failure and Regenerative Medicine, Shanghai East Hospital, Tongji University School of Medicine and Shanghai Institute of Stem Cell Research and Clinical Translation, Shanghai, People's Republic of China

⁴Institute for Stem Cell and Regeneration, CAS, Beijing, People's Republic of China

Correspondence

Huang-Tian Yang, MD, PhD, Laboratory of Molecular Cardiology, Shanghai Institutes of Nutrition and Health, CAS, 320Yue Yang Road, Biological Research Building A, IHS Mail Box 115, Shanghai, 200031, People's Republic of China.

Email: htyang@sibs.ac.cn

Funding information

Science and Technology Commission of Shanghai Municipality; Major Program of Development Fund for Shanghai Zhangjiang National Innovation Demonstration Zone; National Natural Science Foundation of China; Strategic Priority Research Program of the CAS; National Key R&D Program of China

Abstract

Acute myocardial infarction (MI) resulting from coronary ischemia is a major cause of disability and death worldwide. Transplantation of human embryonic stem cell (hESC)-derived cardiovascular progenitor cells (hCVPCs) promotes the healing of infarcted hearts by secreted factors. However, the hCVPC-secreted proteins contributing to cardiac repair remain largely unidentified. In this study, we investigated protective effects of neurotrophin (NT)-3 secreted from hCVPCs in hearts against myocardial ischemia/reperfusion (I/R) injury and explored the underlying mechanisms to determine the potential of using hCVPC products as a new therapeutic strategy. The implantation of hCVPCs into infarcted myocardium at the beginning of reperfusion following 1 hour of ischemia improved cardiac function and scar formation of mouse hearts. These beneficial effects were concomitant with reduced cardiomyocyte death and increased angiogenesis. Moreover, hCVPCs secreted a rich abundance of NT-3. The cardioreparative effect of hCVPCs in the I/R hearts was mimicked by human recombinant NT-3 (hNT-3) but canceled by NT-3 neutralizing antibody (NT-3-Ab). Furthermore, endogenous NT-3 was detected in mouse adult cardiomyocytes and its level was enhanced in I/R hearts. Adenovirus-mediated NT-3 knockdown exacerbated myocardial I/R injury. Mechanistically, hNT-3 and endogenous NT-3 inhibited I/R-induced cardiomyocyte apoptosis through activating the extracellular signal-regulated kinase (ERK) and reducing the Bim level, resulting in the cardioreparative effects of infarcted hearts together with their effects in the

Wei Bi and Jinxi Wang contributed equally to this study.

This is an open access article under the terms of the Creative Commons Attribution-NonCommercial-NoDerivs License, which permits use and distribution in any medium, provided the original work is properly cited, the use is non-commercial and no modifications or adaptations are made.

© 2021 The Authors. STEM CELLS TRANSLATIONAL MEDICINE published by Wiley Periodicals LLC on behalf of AlphaMed Press

improvement of angiogenesis. These results demonstrate for the first time that NT-3 is a cardioprotective factor secreted by hCVPCs and exists in adult cardiomyocytes that reduces I/R-induced cardiomyocyte apoptosis via the ERK-Bim signaling pathway and promotes angiogenesis. As a cell product, NT-3 may represent as a noncell approach for the treatment of myocardial I/R injury.

KEYWORDS

apoptosis, cardiac repair, ERK-Bim signaling pathway, human embryonic stem cell-derived cardiovascular progenitor cells, neurotrophin-3

1 | INTRODUCTION

Acute myocardial infarction (MI) resulting from coronary ischemia is a major cause of disability and death worldwide. Following MI, dead cardiomyocytes are replaced by fibrous scar tissue, causing ventricular remodeling and development of heart failure (HF).^{1,2} To rescue ischemic myocardium and limit infarct size, timely and effective reperfusion in MI patients is the current therapeutic choice, however, this can cause additional damage, termed as ischemia/reperfusion (I/R) injury.^{3,4} Therefore, identifying ways to protect cardiomyocytes against I/R injury during the early stage of reperfusion and clarifying the underlying protective mechanisms are necessary to promote the development of new therapeutic approaches for the treatment of ischemic heart disease.

Cell therapy by transplantation of stem/progenitor cells and their derived cardiovascular cells is a promising therapeutic approach for the treatment of ischemic heart disease.⁵⁻¹³ Among the various transplantable cells, cardiac lineage cells derived from human pluripotent stem cells (hPSCs), including human embryonic stem cells (hESCs) and human induced pluripotent stem cells (hiPSCs), show great potential in promoting healing of infarcted hearts.^{5,7,13-17} Implantation of hESC-derived cardiovascular progenitor cells (hCVPCs) during the subacute stage of I/R has been shown to improve cardiac function in rodent infarcted hearts⁶ and increase engraftment in the infarcted myocardium of immunosuppressed nonhuman primates.¹⁸ Moreover, no complications of arrhythmias, tumor formation, or immunosuppression-related adverse events have been observed in the patients with advanced ischemic HF when SSEA1⁺ hCVPCs are transplanted.⁵ Recently, we demonstrated that transplantation of SSEA1⁺ hCVPCs^{19,20} at the acute-phase of MI significantly reduces cardiomyocyte death, improves the recovery of left ventricular (LV) function, and/or limits the scar size in the murine infarcted hearts¹⁵ and nonhuman primate MI models.⁷ The beneficial effects of hCVPCs to the infarcted hearts are associated with paracrine factors, such as microRNAs^{21,22} and long noncoding RNA MALAT1²³ in their secreted extracellular vesicles (EVs). Recently, we identified that hCVPC-secreted cytokines, interleukin-4 and interleukin-13, modulate macrophage polarization toward a reparative phenotype in the

Significance statement

While implantation of human embryonic stem cell-derived cardiovascular progenitor cells (hCVPCs) can promote the recovery of infarcted hearts via paracrine action, the contribution of secreted factors remains identified. The present study has revealed that neurotrophin (NT)-3 is highly secreted by hCVPCs and the level is enhanced during mouse myocardial ischemia/reperfusion (I/R) injury. Injection of NT-3 mimics the beneficial effect of hCVPCs in I/R hearts via suppressing cardiomyocyte apoptosis through modulation of the ERK-Bim signaling pathway and promoting angiogenesis. These findings uncover a new function of NT-3 in hCVPCs and I/R hearts and indicate a potential therapeutic role for cell products in the treatment of ischemic heart disease.

infarcted hearts via activation of a signal transducer and activator of transcription 6.¹⁵ However, it is unclear whether other proteins secreted from hCVPCs may exert synergistic cardioreparative effects, especially with respect to improving the cardiomyocyte survival during early reperfusion following myocardial ischemia.

Neurotrophins (NTs) are a family of highly conserved growth factors that serve a diverse set of functions in the nervous system²⁴ and cardiovascular cells.^{25,26} NT-3, a member of the neurotrophin family,²⁷ and its tropomyosin kinase receptor C (TrkC) are expressed in cardiovascular cells.^{25,28} Genetic deficiency of *Nt3* causes atrial and ventricular septal defects in mice.²⁹ In primary-cultured neonatal rat cardiomyocytes (NRCMs), NT-3 increases the mRNA level of cardiac hypertrophic genes and cell size, but it is downregulated in rat cardiac hypertrophy induced by pressure overload *in vivo* and in NRCMs stimulated by endothelin-1.²⁸ In addition, adenovirus-overexpression of NT-3 stimulates the proliferation of capillary endothelial cells in the murine ischemic hind limbs via activation of protein kinase B (PKB/Akt) and endothelial nitric oxide synthase.^{25,26} However, it is unknown whether NT-3 is a paracrine factor of hCVPCs and little is known about the dynamic expression pattern and functions of NT-3 in the adult heart with myocardial I/R injury.

The present study used a murine myocardial I/R model with injection of SSEA1⁺ hCVPCs into infarcted myocardium at the onset of reperfusion, combined with *in vivo* and *in vitro* manipulation of NT-3 levels

and extracellular signal-regulated kinase (ERK) activation to investigate (i) the effects of hCVPCs on infarct healing when intramyocardially injected at the onset of reperfusion; (ii) the endogenous levels of NT-3

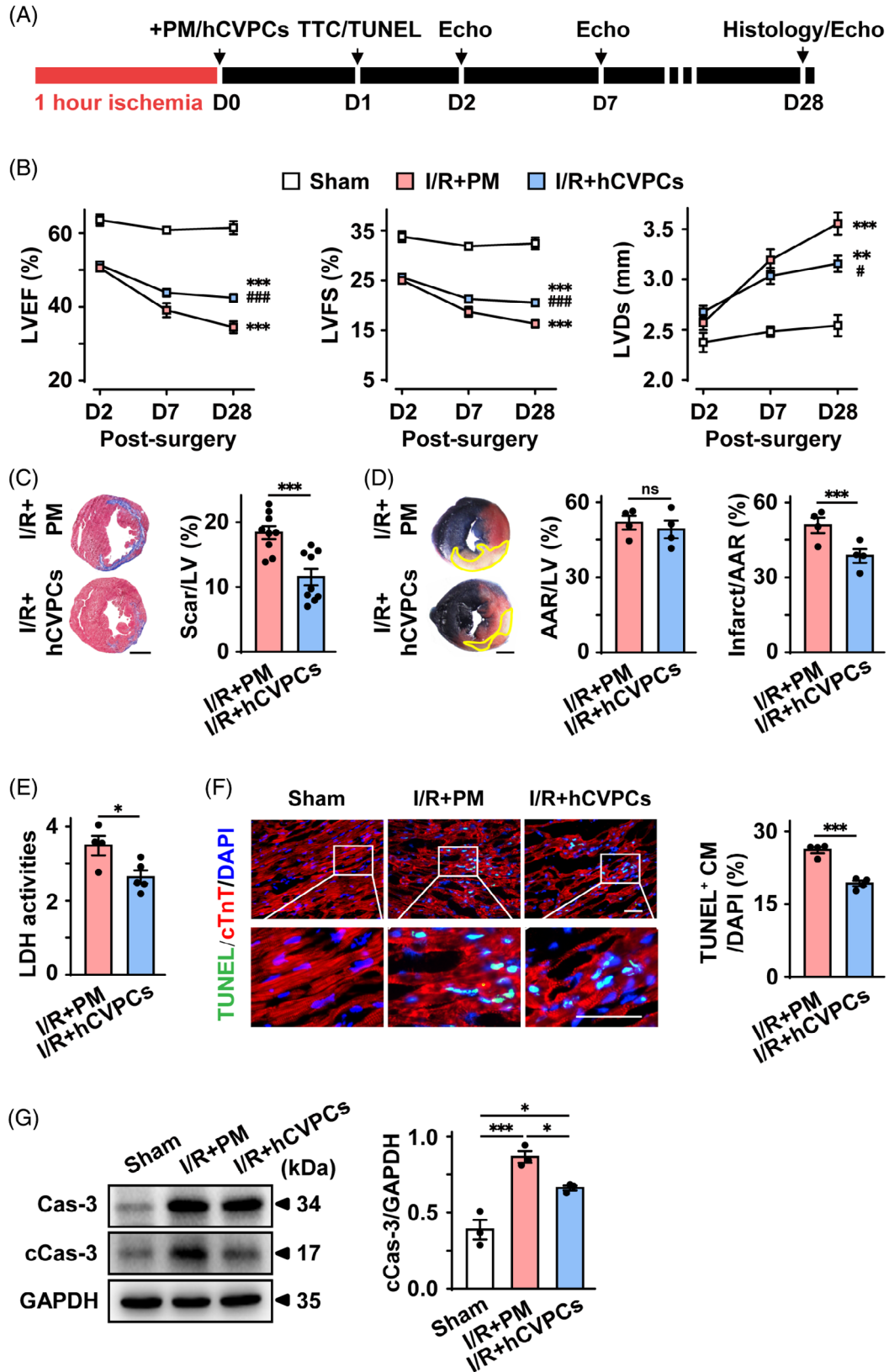


FIGURE 1 Legend on next page.

protein in the adult murine hearts with and without myocardial I/R and its role in myocardial I/R injury; (iii) the signaling pathways mediated by NT-3 in the protection of cardiomyocytes from I/R injury; and (iv) the contribution of NT-3 to the beneficial effects of hCVPCs in promoting the healing of I/R hearts. Our findings have revealed a previously unrecognized paracrine factor of hCVPCs, its expression pattern and function in I/R hearts, the contribution to the cardioreparative effects of hCVPCs, and the underlying mechanisms. These findings not only provide new insights into the roles and mechanisms of the neurotrophin family member in tissue repair but also enrich our understanding of how hPSC-derived cardiac lineage cells promote repair of the infarcted heart.

2 | MATERIALS AND METHODS

2.1 | Animals

Adult male C57BL/6 mice (The Shanghai Slac Laboratory Animal Co. Ltd, Shanghai, China) were used in the experiments. All procedures involving animals were performed in accordance with the Guidelines for Care and Use of Laboratory Animals published by the US National Institutes of Health (NIH Publication, 8th Edition, 2011) and approved by the Institutional Animal Care and Use Committee of Shanghai Institutes for Biological Sciences and Shanghai Institute of Nutrition and Health (Shanghai, China).

2.2 | Induction of hCVPCs and preparation of hCVPC-conditioned medium

The induction of hCVPCs was conducted following the protocol reported previously.^{7,19,20} Detailed experimental methods are available in the Supplemental Materials section.

2.3 | Flow cytometer analysis

Flow cytometer analysis was performed as described previously.^{7,19,20} Detailed experimental methods are available in the Supplemental Materials section.

2.4 | Immunocytochemical staining analysis

Cells were immunostained as described previously.^{7,19,20} Detailed experimental methods are available in the Supplemental Materials section.

2.5 | Myocardial I/R injury model and study designs

The myocardial I/R model was induced as previously described.³⁰ Briefly, male C57BL/6 mice at 10-12 weeks-old were anesthetized via intraperitoneal injection (i.p.) of 50 mg/kg sodium pentobarbital and mechanically ventilated using a volume regulated respirator (SAR830, Cwe Incorporated). Body temperature was maintained at 37°C throughout the surgical procedure. Ischemia was produced through ligation of the left anterior descending (LAD) coronary artery with an 8-0 Prolene suture, while Sham group mice had a loose suture placed in the same position. After 1 hour of occlusion, the ligature was released and various treatments were performed at the onset of reperfusion in the following groups: (i) for effects of hCVPCs in I/R hearts, Sham group, I/R + Puramatrix (PM, reported to retain the transplanted cells or proteins in the injected site,^{31,32} 3-D Matrix, Ltd) control group (10 μ L 10% sucrose solution+10 μ L 0.4% PM/heart), and I/R + hCVPC group (5×10^5 cells in 20 μ L of 0.2% PM/heart). The PM and hCVPCs were injected into the peri-infarct regions of I/R hearts at 3 sites; (ii) for functions of NT-3 in I/R hearts, I/R + PBS (phosphate-buffered saline, 20 μ L/heart) group or I/R + hNT-3 (human recombinant NT-3) group (0.5 μ g in 20 μ L PBS/heart, GeneTex). PBS or hNT-3 was injected into the peri-infarct regions at 3 sites, followed by continuous release of PBS or hNT-3 (0.5 μ g d⁻¹) for up to 1 week via the Micro-Osmotic Pump (Model 1004, Alzet) implanted subcutaneously; (iii) for involvement of the ERK-Bim signaling pathway in NT-3-regulated cardioprotection, I/R group, I/R + hNT-3 group (0.5 μ g in 20 μ L/heart), I/R + SCH (ERK specific inhibitor SCH772984, Selleck) group, and I/R + hNT-3 + SCH group. hNT-3 was intramyocardially injected and SCH772984 (10 μ g/20 μ L/heart) was administered (i.p.) at the onset of reperfusion; (iv) and for contributions of NT-3 to the benefits of hCVPCs in I/R hearts, Sham group, I/R group (PM control), I/R + IgG (mouse immunoglobulin G, R&D) group, I/R + NT-3-Ab (NT-3-neutralizing antibody, R&D) group, I/R + hCVPCs group, I/R + hCVPCs+IgG group, and I/R + hCVPCs+NT-3-Ab group. IgG or NT-3-Ab at 300 ng/mL was intramyocardially injected together with hCVPCs (5×10^5 cells/heart) or PM into the peri-infarct region at 3 sites (20 μ L/heart). Hearts were harvest at day 1 or day 28 after I/R for analysis.

2.6 | Echocardiography

Transthoracic echocardiography (Vevo 2100, Visual Sonics) with a 25 MHz imaging probe was used on to obtain serial ultrasound images

FIGURE 1 hCVPC delivery improves cardiac function and cardiomyocyte survival in ischemia/reperfusion (I/R) hearts. A, Schematic of hCVPC transplantation and analysis. B, Left ventricle (LV) ejection fraction (LVEF), LV fractional shortening (LVFS) and LV systolic dimension (LVDs) measured by echocardiography (Echo). n = 10. C, Representative cross-sectional images and quantitative data of heart scar area stained with Masson's trichrome at day 28 post-I/R. n = 9. Scale bars = 1 mm. D, Representative and quantification of 2,3,5-triphenyltetrazoliumchloride (TTC)/Evans blue staining for infarct size in the hearts at day 1 post-I/R. n = 4. Scale bar = 1 mm. E, Fold changes of lactate dehydrogenase (LDH) activities in PM (Puramatrix) and hCVPCs groups compared with the one in Sham mice. n = 4-5. F, Representative and quantification of immunohistochemical (IHC) staining for terminal deoxynucleotidyl transferase dUTP nick end labeling positive (TUNEL⁺) cardiomyocytes in the infarct and border zones of hearts at day 1 post-I/R. n = 4. Scale bar = 50 μ m. G, Representative and averaged Western blot analysis for caspase-3 (Cas-3), cleaved Cas-3 (cCas-3) and GAPDH in the infarct and border zones of hearts at day 1 post-I/R. n = 3. *P < .05, **P < .01, ***P < .001 vs the Sham group; #P < .05, ###P < .001 vs the I/R + PM group. ns, nonsignificant

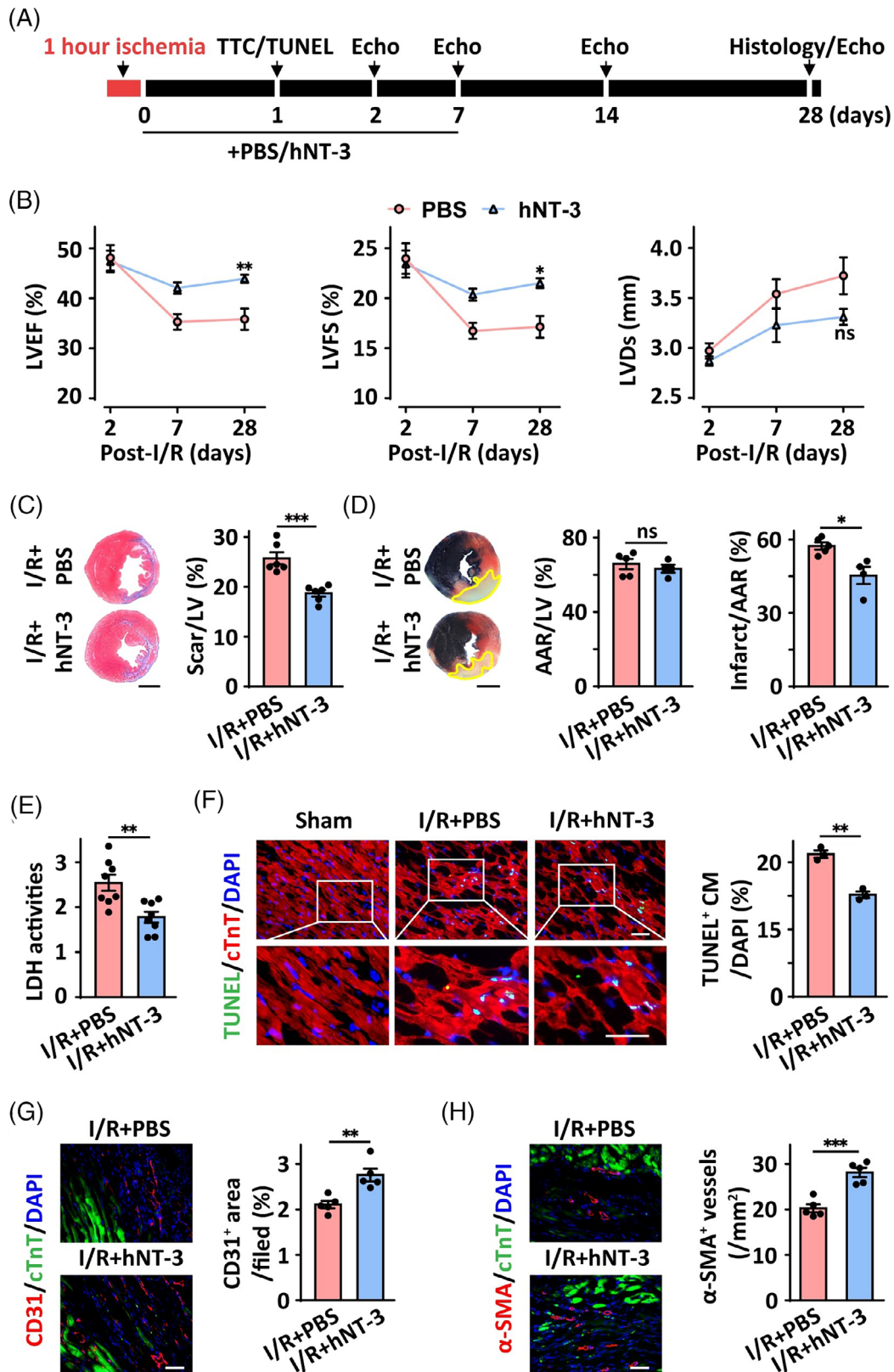


FIGURE 2 Exogenous hNT-3 promotes infarct healing of I/R hearts. A, Schematic of hNT-3 treatment regime in C57BL/6 wild type (WT) I/R mice. B, LVEF, LVFS and LVDs measured by echocardiography. $n = 9$. C, Representative cross-sectional images and quantitative data of scar area stained with Masson's trichrome at day 28 post-I/R. $n = 6$. Scale bars = 1 mm. D, Representative and quantification of TTC/Evans blue staining for infarct size in the hearts at day 1 post-I/R. $n = 4-5$. Scale bar = 1 mm. E, Fold changes of LDH activities in LV serum between I/R + PBS and I/R + hNT-3 group compared with Sham mice. $n = 8$. F, Representative and quantification of IHC staining for TUNEL⁺ cardiomyocytes in the infarct and border zones of hearts at day 1 post-I/R. $n = 3$. Scale bar = 50 μm . G, IHC staining and quantitative data for CD31⁺ endothelial cells in the infarct and border zones at day 28 post-I/R. $n = 5$. Scale bar = 50 μm . H, IHC staining and quantitative data for α -smooth muscle actin positive (α -SMA⁺) blood vessels in the infarct and border zones at day 28 post-I/R. Scale bar = 50 μm . * $P < .05$; ** $P < .01$; *** $P < .001$; ns, nonsignificant

in the anesthetized mice as previously described.^{15,23} LV ejection fraction (LVEF), LV fractional shortening (LVFS), and LV systolic dimension (LVDs) were measured using the M-mode at day 2, 7 and 28 after surgery. All measurements were averaged from three consecutive cardiac cycles in a blinded manner.

2.7 | Construction of recombinant adenovirus

Recombinant adenoviruses (Ad) expressing short hairpin RNA were prepared as reported previously.^{30,33,34} Detailed experimental methods are available in the Supplemental Materials section.

2.8 | Adenovirus-mediated gene delivery in vivo

Surgical procedures and adenoviral delivery were carried out as previously described.^{30,34} Briefly, the surgery process was the same as described above and a 30-gauge needle containing 30 μ L of diluted the scramble (sh-scramble/negative control, shNC) or the short hairpin RNA against mouse NT-3 (shNT-3) (3×10^{10} pfu/mL) was injected into the myocardium of LV at 3 sites. The efficiency of adenoviral downregulation of NT-3 was assessed by Western blot at day 4 after adenovirus injection. The same mice were then subjected to myocardial I/R surgery.

2.9 | Immunohistochemical staining

Immunohistochemical (IHC) analysis was performed as previously described.^{15,23} Detailed experimental methods are available in the Supplemental Materials section.

2.10 | Terminal deoxynucleotidyl transferase dUTP nick end labeling staining

Terminal deoxynucleotidyl transferase dUTP nick end labeling (TUNEL) positive (TUNEL⁺) cardiomyocytes in I/R hearts and isolated cells were evaluated using an In situ Cell Death Detection Kit (Roche Applied Science, Germany), co-stained with anti-cTnT antibody. The percentage of TUNEL⁺ cardiomyocytes was blindly quantified as the ratio of TUNEL⁺cTnT⁺ cardiomyocytes to the total cTnT⁺ cells as described previously.^{15,23}

2.11 | Analysis of infarct size

Infarct size was measured by using 1% w/v of 2, 3, 5-triphenyltetrazolium chloride (TTC, T8877, Sigma-Aldrich) as previously described.³⁰ Detailed experimental methods are available in the Supplemental Materials section.

2.12 | Masson's trichrome staining and FITC-conjugated wheat germ agglutinin staining

Heart frozen sections were stained after 28 days of reperfusion with Masson's trichrome as previously described.^{15,23} Briefly, morphometric parameters measured on five sections each heart, including total LV area and scar area, were blindly analyzed from ligated to apical position of the heart and the scar size was calculated as the total scar area divided by the LV area with Image J. The FITC-labeled wheat germ agglutinin antibody (1:100, Sigma, L4895) was used to perform immunostaining on LV cross sections from the same level of various hearts. The images at each section were captured by Zeiss fluorescence microscope and 60-90 myocytes from 2-3 independent fields per section in each heart were quantified using Image J as reported previously.^{14,35}

2.13 | Lactate dehydrogenase activity

Lactate dehydrogenase (LDH) activity was analyzed with an LDH Cytotoxicity Assay Kit (Beyotime Institute of Biotechnology) according to the supplier's instructions as previously described.^{34,36} Detailed experimental methods are available in the Supplemental Materials section.

2.14 | Isolation and culture of adult mouse cardiomyocytes and adult mouse cardiac fibroblasts

Adult mouse cardiomyocytes (AMCMs) were isolated from the hearts of adult male C57BL/6 mice and cultured as previously described.³⁰ Detailed experimental methods are available in the Supplemental Materials section.

2.15 | Simulated I/R in isolated AMCMs

A cellular simulated I/R (sI/R) injury model was used for isolated AMCMs as previously reported.^{37,38} Briefly, isolated AMCMs were incubated with ischemic buffer for 1 hour, followed by 1 hour of reperfusion using culture medium in 21% O₂ and 5% CO₂. The various treatments were started at the beginning of reperfusion lasting for 1 hour. Detailed experimental methods are available in the Supplemental Materials section.

2.16 | Western blot protein array analysis

Total proteins from the infarct and border zones of LV tissues or AMCMs were extracted and analyzed as previously reported.^{15,23,30,39} Detailed experimental methods are available in the Supplemental Materials section.

2.17 | Quantitative reverse transcription polymerase chain reaction

Quantitative reverse transcription polymerase chain reaction (RT-qPCR) was performed as described previously.^{15,19,23} Detailed experimental method is available in the Supplemental Materials section.

2.18 | Statistical analysis

Data are presented as mean \pm SEM. Statistical significance was analyzed by using unpaired Student's *t*-test for comparisons between two groups, one-way analysis of variance (ANOVA) for comparisons between more than two groups when there was one independent variable, and two-way ANOVA for the analysis of two independent variables or echocardiographic data. One-way and two-way ANOVA were followed with Bonferroni's multiple comparison. Statistically analysis was performed with Graphpad Prism software (version 6.1). A *P*-value $< .05$ was considered statistically significant.

3 | RESULTS

3.1 | Therapeutic benefits of hCVPCs in mice with myocardial I/R injury

The H9 hESCs (WiCell)-generated SSEA1⁺ hCVPCs displayed CVPC markers MESP1, ISL1, MEF2C, GATA4, and NKX2.5 (Figure S1) as previously reported.^{7,15,19,20,23} Mice injected with hCVPCs in the peri-infarct region at the onset of reperfusion following 1 hour of ischemia (Figure 1A) showed comparable LVEF, LVFS and LVDs with those of the I/R group at day 2 post-I/R, whereas the hCVPC treatment significantly improved these parameters that were worsened in the I/R control group during the 4-week follow-up period (Figure 1B). Consistently, Masson's trichrome staining analysis at day 28 post-I/R showed that scar size in the hCVPC-treated hearts was significantly smaller than the control group (Figure 1C). As the reduction of scar size may partially result from a reduction in cell death and/or improvement of angiogenesis, we analyzed infarct size and apoptotic cardiomyocytes at day 1 post-I/R. The I/R-PM and hCVPC groups showed comparable area at risk (AAR) to LV, but the infarct area (Figure 1D), serum LDH activity (an index of cell death, Figure 1E), and TUNEL⁺ cardiomyocytes (Figure 1F) were significantly attenuated in the hCVPC group compared with those in the PM group. Moreover, the I/R-increased cleaved caspase-3 (cCas-3) in the infarct and border zones was reduced in the hCVPC treated group (Figure 1G). IHC staining at day 28 post-I/R showed an increased number of CD31⁺ endothelial cells (Figure S2A) and α -smooth muscle actin positive (α -SMA⁺) vessels (Figure S2B) in the infarct and border zones of hCVPC-treated I/R hearts compared with the PM group.

3.2 | NT-3 is highly secreted from hCVPCs and promotes infarct healing of I/R hearts

To determine whether the beneficial effects of hCVPCs on cardiovascular cells in the I/R hearts are related to the paracrine action of hCVPCs, the hCVPC-secretome was analyzed as previously described.¹⁵ Among the secreted proteins of hCVPCs, an abundance of NT-3 was detected in the hCVPCs and preparation of hCVPC-conditioned medium (hCVPC-CdM) (Figure S3A). This was confirmed by RT-qPCR (Figure S3B) and ELISA analysis (Figure S3C). To determine the role of exogenous NT-3 in the I/R hearts, hNT-3 (0.5 μ g/20 μ L) was then injected into the peri-infarct region of the I/R hearts at the beginning of reperfusion followed by continuous subcutaneous administration of NT-3 (0.5 μ g d⁻¹) up to day 7 of I/R (Figure 2A). LVEF, LVFS, and LVDs were comparable between the PBS and hNT-3-injected groups without I/R insult (Figure S4) or at day 2 post-I/R, whereas hNT-3 treatment improved LVEF and LVFS in the I/R hearts during the 4-week follow-up period (Figure 2B). Concurrently, I/R hearts developed smaller infarct scars (Figure 2C) and less myocyte hypertrophy (Figure S5) in the hNT-3-treated group than those in the control group. Moreover, the AAR of LV at day 1 post-reperfusion was comparable between the PBS and hNT-3 treatment groups, whereas the infarct size (Figure 2D), LDH release (Figure 2E), the number of TUNEL⁺ cardiomyocytes in the infarct and border zones (Figure 2F), and cCas-3 (Figure S6) were significantly reduced in the hNT-3 group. Furthermore, the number of CD31⁺ endothelial cells (Figure 2G) and the density of SMA⁺ blood vessels in the infarct and border zones (Figure 2H) were higher in the hNT-3-treatment group than those in the PBS control group at day 28 post-I/R.

3.3 | Exogenous hNT-3 protects the cardiomyocytes from sl/R injury

To determine whether the cardioprotective effects of hNT-3 are related to its action in the cardiomyocytes, we induced sl/R injury in the AMCMs as reported previously.^{37,38} Notably, the sl/R injury-induced cardiomyocyte death (in round shape, Figure 3A) and LDH release (Figure 3B) at the 1 hour of reperfusion were decreased by hNT-3 in a concentration-dependent manner. Concomitantly, hNT-3 at 10 ng/mL significantly decreased the number of TUNEL⁺ AMCMs (Figure 3C) and the cCas-3 level (Figure 3D) induced by sl/R injury.

3.4 | NT-3 is an endogenous protective factor in the heart against I/R injury

To determine whether NT-3 exists in the adult murine hearts and contributes to the alleviation of myocardial I/R injury, NT-3 was knocked down in the heart by intramyocardial injection of Ad-shNT-3 at 4 days before the myocardial I/R (Figure 4A). NT-3 protein was detected in isolated AMCMs and adult mouse cardiac fibroblasts (AMCFs)

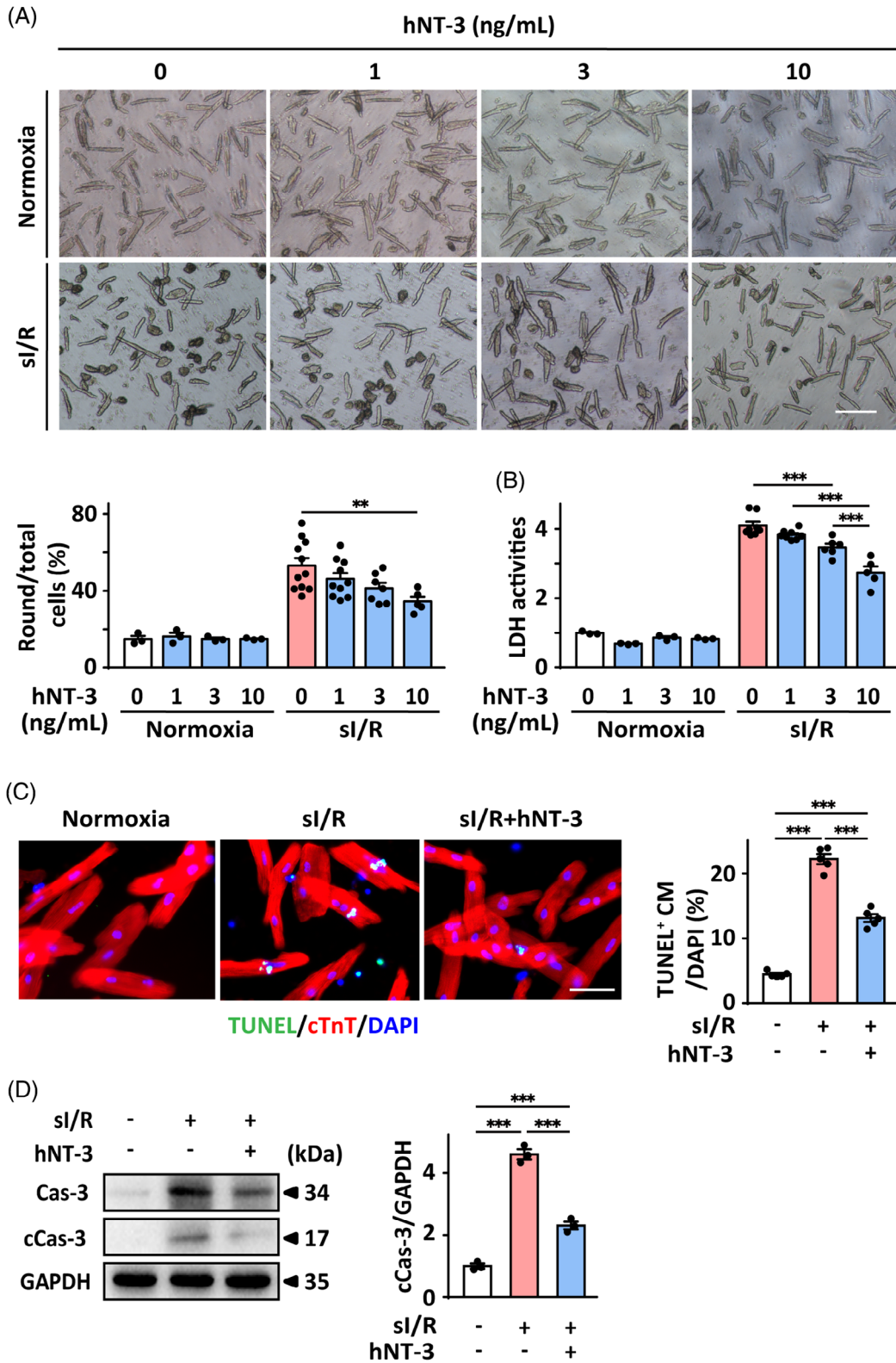


FIGURE 3 Protective effects of exogenous hNT-3 in the adult mice cardiomyocytes (AMCMs) subjected to 1 hour of simulated I/R (si/R) injury. A, Representative images of AMCM morphology and quantitative percentages of round/total cells at normoxia or 1-hour post-si/R. n = 5-11. Scale bar = 100 μ m. B, LDH activities in AMCM culture media. n = 5-8. C, Representative and quantification of IHC staining for TUNEL⁺ AMCMs. n = 5. Scale bar = 50 μ m. D, Representative and averaged Western blot analysis in AMCMs at 1-hour post-si/R. n = 3. **P < .01; ***P < .001

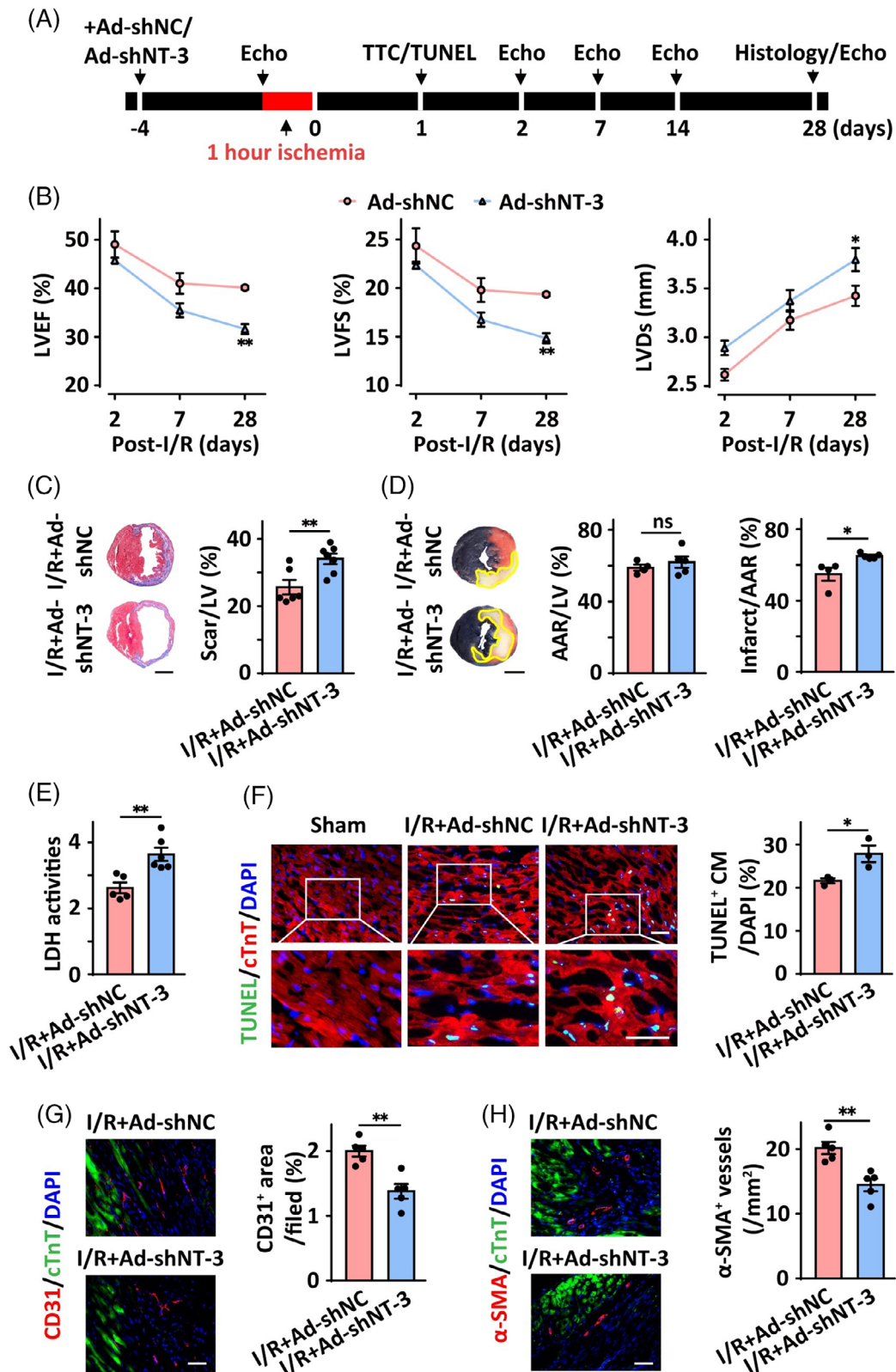


FIGURE 4 NT-3 is an endogenous protective factor in the heart against I/R injury. A, Schematic of treatment regime in I/R mice. B, LVEF, LVFS and LVDs measured by echocardiography. $n = 9$. C, Representative cross-sectional images and quantitative data of scar area stained with Masson's trichrome at day 28 post-I/R. $n = 6-7$. Scale bars = 1 mm. D, Representative and quantification of TTC/Evans blue staining for the infarct size at day 1 post-I/R. $n = 4-5$. Scale bar = 1 mm. E, Fold changes of LDH activities in the LV serum at day 1 of I/R. $n = 5-6$. F, Representative and quantification of IHC staining for TUNEL⁺ cardiomyocytes in border and infarct zones of hearts at day 1 post-I/R. $n = 3$. Scale bar = 50 μm . G, IHC staining and quantitative data for CD31⁺ endothelial cells in the infarct and border zones at day 28 post-I/R. $n = 5$. Scale bar = 50 μm . H, IHC staining and quantitative data for $\alpha\text{-SMA}^+$ blood vessels in the infarct and border zones at day 28 post-I/R. $n = 5$. Scale bar = 50 μm . Ad-shNC, adenovirus-short hairpin RNA of negative control; Ad-shNT-3, adenovirus-short hairpin RNA of mouse NT-3. * $P < .05$; ** $P < .01$ vs the Ad-shNC group or as indicated in figures; ns, nonsignificant

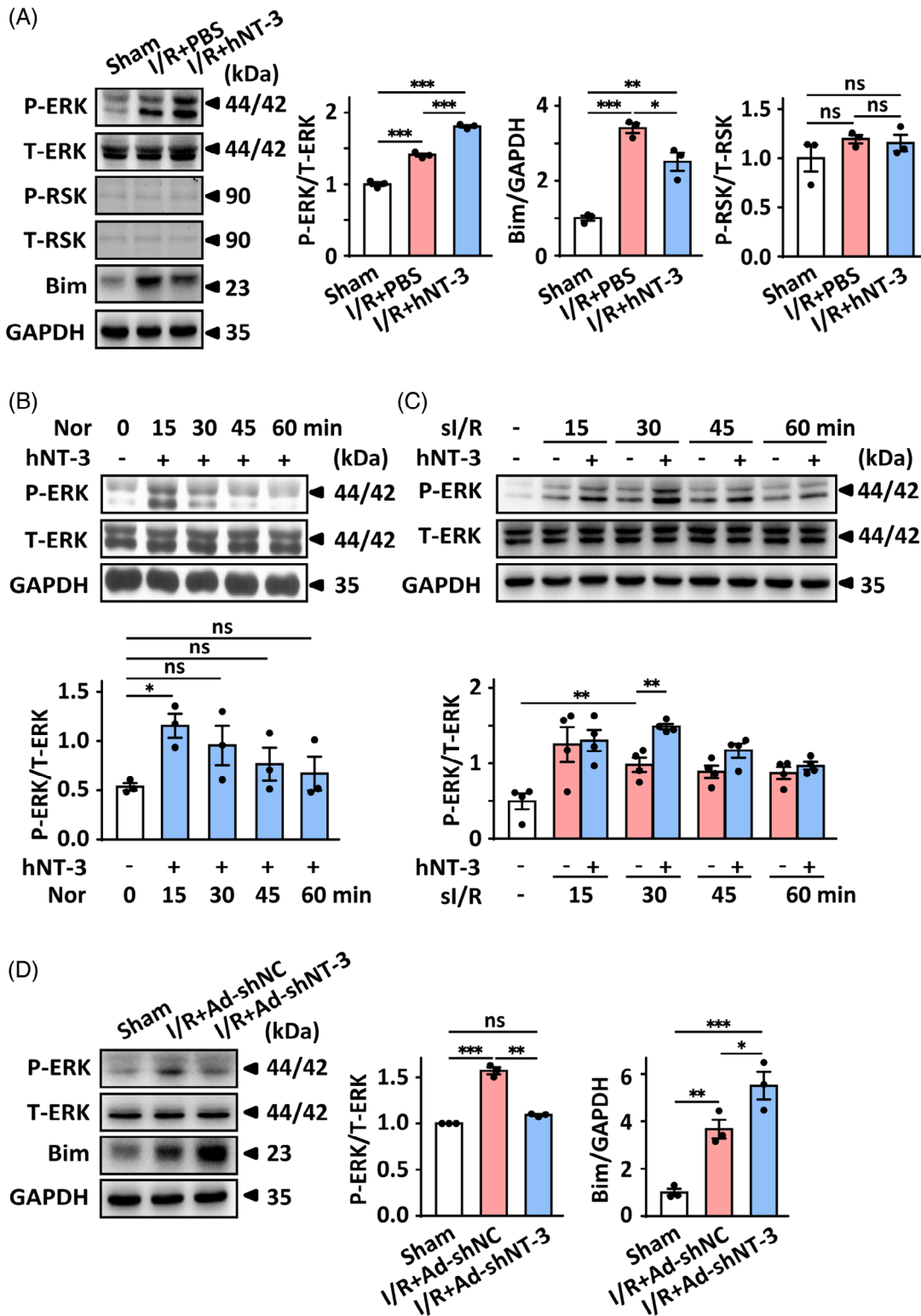


FIGURE 5 NT-3 activates phosphorylation of ERK in the I/R hearts and AMCMs. A, Representative and averaged Western blot analysis in the mice hearts at 1 day post-I/R. n = 3. B, Representative and averaged Western blot analysis in the normoxic AMCMs with or without 10 ng/mL hNT-3 treatment. n = 3. C, Representative and averaged Western blot analysis in the AMCMs subjected to sl/R injury with or without 10 ng/mL hNT-3 treatments. n = 3. D, Representative and averaged Western blot in the NT-3 knockdown hearts at day 1 post-I/R. n = 3. *P < .05; **P < .01; ***P < .001; ns, nonsignificant

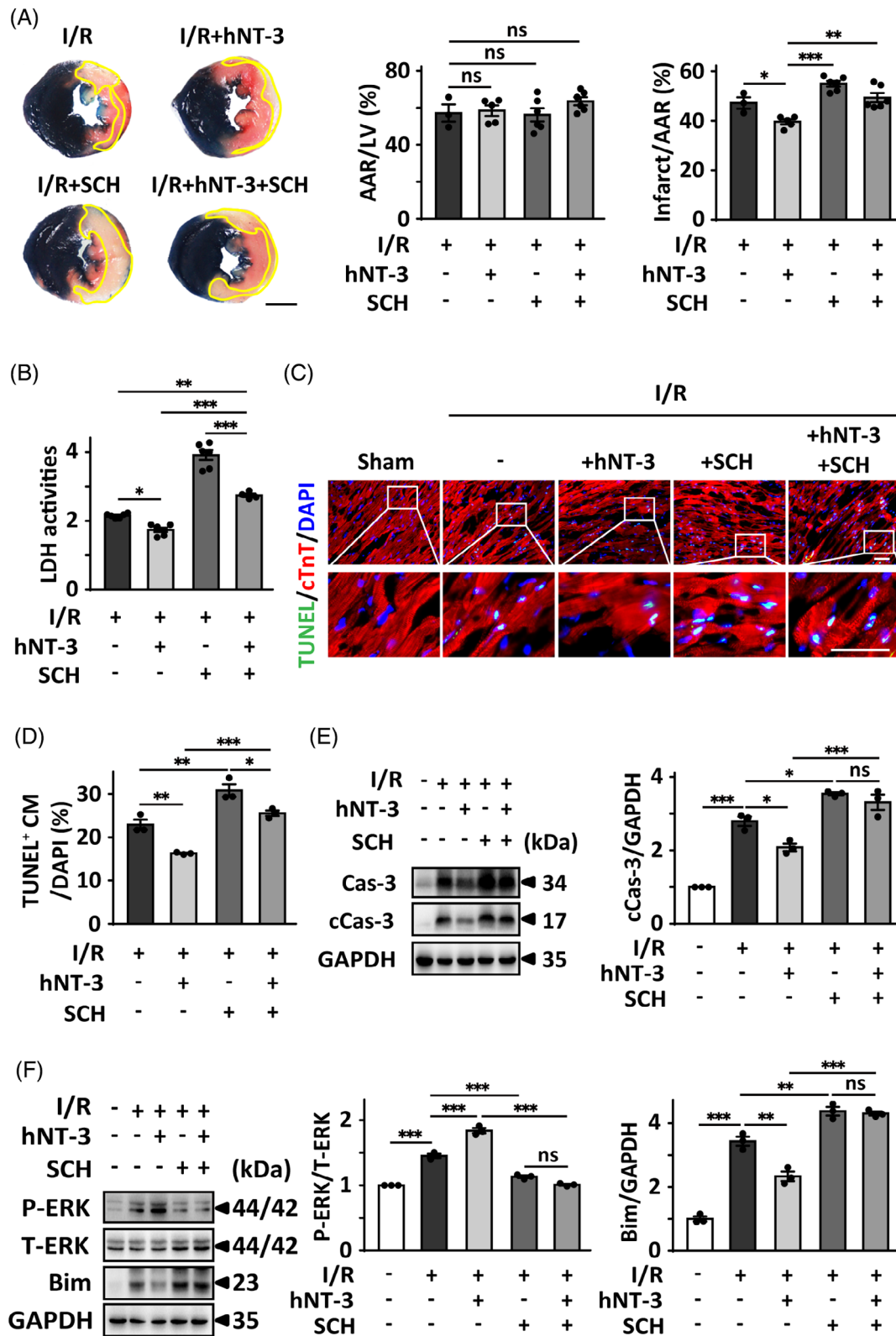


FIGURE 6 NT-3 protects the heart against I/R-induced cardiomyocyte apoptosis via the ERK-Bim signaling pathway. A, Representative and quantification of TTC/Evans blue staining for infarct size in the hearts among I/R, I/R + hNT-3 (0.5 μ g), I/R + SCH (10 μ g) and I/R + hNT-3 + SCH groups at day 1 post-I/R. $n = 3-6$. Scale bar = 1 mm. B, Fold changes of LDH activities in the LV serum compared with the one in Sham mice hearts at day 1 post-I/R. $n = 4-6$. C and D, Representative and quantification of IHC staining for TUNEL⁺ cardiomyocytes in the infarct and border zones of hearts at day 1 post-I/R. $n = 4$. Scale bar = 50 μ m. E and F, Representative and averaged Western blot of various proteins in the infarct and border zones of day 1 post-I/R hearts. $n = 3$. SCH, ERK inhibitor SCH772984. * $P < .05$; ** $P < .01$; *** $P < .001$; ns, nonsignificant

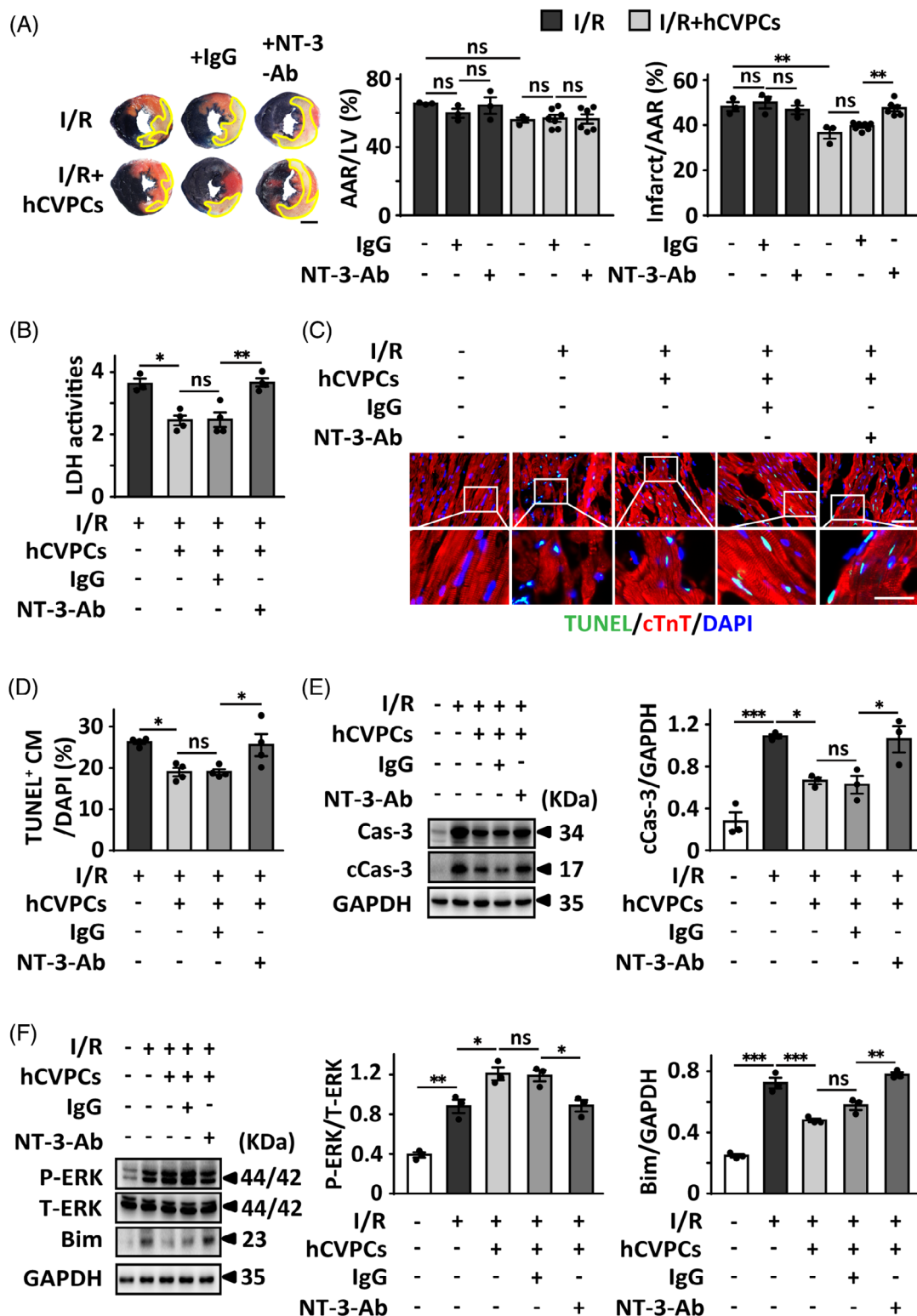


FIGURE 7 NT-3 contributes to the reparative effects of hCVPcs in the I/R hearts via activating the ERK-Bim signaling pathway. A, Representative and quantification of TTC/Evans blue staining for infarct size in the hearts at day 1 post-I/R. n = 3-6. Scale bar = 1 mm. B, LDH activities in the LV serum at day 1 of I/R. n = 3-4. C and D, Representative and quantification of IHC staining for TUNEL⁺ cardiomyocytes in the border zones of infarcted hearts at day 1 post-I/R. n = 4. Scale bar = 50 μ m. E, Representative and averaged Western blot analysis for Cas-3, cCas-3 and GAPDH in the infarct and border zones of day 1 post-I/R hearts. n = 3. F, Representative images and averaged Western blot analysis for P-ERK, T-ERK, Bim, and GAPDH in the infarct and border zones of day 1 post-I/R hearts. n = 3. *P < .05; **P < .01; ***P < .001; ns, nonsignificant

(Figure S7A), whereas levels in the infarct and border zones of I/R hearts decreased at the beginning of reperfusion but significantly increased by day 3 and day 7, and returned to the baseline by day 28 post-reperfusion (Figure S7B). Compared with the Ad-shNC control group, the NT-3 protein level in the LV was downregulated by 30% in the heart by intramyocardial injection of Ad-shNT-3 at 4 days before the myocardial I/R (Figure S8A), whereas the LVEF, LVFS, and LVDs were similar between the two groups at day 4 post-infection before I/R surgery (Figure S8B). At day 2 post-I/R, LVEF, LVFS, and LVDs did not differ between the two groups ($P > .05$), whereas lower LVEF and LVFS were detected in NT-3 knockdown mice at day 28 post-I/R when compared with those of the Ad-shNC mice (Figure 4B). The NT-3 knockdown group had large infarct scars compared with Ad-shNC control mice at day 28 after I/R (Figure 4C). Moreover, larger infarct scars (Figure 4D), higher LDH release (Figure 4E), increased TUNEL⁺ cardiomyocytes (Figure 4F) and cCas-3 (Figure S8C) in the infarct and border zones at day 1 of I/R were detected in the NT-3 knockdown mice compared with those in the Ad-shNC control groups, though they had comparable AAR to LV (Figure 4D). The Ad-shNT-3 group showed a lower number of CD31⁺ endothelial cells (Figure 4G) and lower density of α -SMA⁺ blood vessels (Figure 4H) in the infarct and border zones of I/R hearts than those in the Ad-shNC control group. These data support our hypothesis that NT-3 is an endogenous protective factor in the heart against I/R injury.

3.5 | NT-3 protects cardiomyocytes from I/R-induced apoptosis via activating ERK-Bim signaling pathway

Then the levels of phosphokinases involved in the regulation of cell survival were compared between the PBS- and hNT-3-treated I/R hearts. Among the 43 screened phosphokinases, hNT-3-treatment enhanced the I/R-increased phosphorylation of ERK (P-ERK) in 1 day post-I/R hearts (Figure S9A). The hNT-3-increased P-ERK levels (Figure 5A) but not phosphorylation of Akt and P38 (Figure S9B) at 1 day post-I/R, which was confirmed using Western blot analysis. Myocardial I/R-enhanced protein level of Bim (a downstream target of P-ERK and an activator of mitochondrial apoptosis⁴⁰) was significantly reduced by hNT-3, whereas the phosphorylation of RSK (a P-ERK downstream effector suppressing apoptosis⁴¹) remained unchanged (Figure 5A). Activation of ERK by hNT-3 was further confirmed in AMCMs without sl/R (Figure 5B) or suffering 30 minutes of reperfusion following 1 hour of simulated ischemia (Figure 5C). Moreover, the myocardial I/R-enhanced P-ERK was reversed to the level as seen in the sham group following NT-3 knockdown in the I/R hearts (Figure 5D). To further confirm whether NT-3-mediated inhibition in cardiomyocyte apoptosis via activation of the ERK-Bim signaling pathway, a ERK specific inhibitor SCH772984 was injected intraperitoneally in mice at the onset of reperfusion. SCH772984 inhibited the hNT-3-enhanced ERK phosphorylation level at 10 μ g/20 μ L (Figure S10). Concomitantly, the AAR to LV was comparable among various groups, whereas SCH772984 enlarged the infarct

size compared with the control group and canceled the protective effect of hNT-3 in the limitation of infarct size (Figure 6A). Moreover, I/R-induced LDH activity in serum (Figure 6B), TUNEL⁺ cardiomyocytes in the infarct and border zones (Figure 6C,D), and cCas-3 (Figure 6E) were increased following SCH772984 treatment; and the protective effects of NT-3 on these parameters were reversed by SCH772984 at day 1 post-reperfusion. hNT-3 enhanced P-ERK at day 1 post-reperfusion was blocked by SCH772984 with the oppositely altered levels of Bim (Figure 6F).

The involvement of ERK-Bim signaling pathway in the protection of NT-3 was then confirmed on AMCMs subjected to sl/R injury. SCH772984 decreased sl/R- and hNT-3-enhanced P-ERK levels in a concentration-dependent manner (Figure S11A). Concomitantly, SCH772984 cancelled the hNT-3-afforded protection in the reduction of sl/R-increased round cell proportion (Figure S11B), increased protein levels of Bim, and cCas-3 (Figure S11C).

3.6 | NT-3 contributes to the reparative effects of hCVPCs in I/R hearts via activating the ERK-Bim signaling pathway

Next, we determined whether NT-3 contributes to the cardioreparative effect of hCVPCs by neutralization of NT-3 with its antibody (Figure S12). sl/R-induced increase of LDH activity AMCMs was significantly suppressed by hCVPC-CdM, whereas this protection was cancelled by NT-3-Ab in a concentration-dependent manner but not the IgG control (Figure S12). Furthermore, hCVPCs were injected together with the IgG or NT-3-Ab into the peri-infarct region of I/R hearts. The ratios of AAR to LV were comparable among the various groups, whereas the hCVPC-reduced infarct size at day 1 post-I/R was reversed by the NT-3-Ab but not the IgG control (Figure 7A). Similar changes of serum LDH activity at day 1 reperfusion were observed (Figure 7B). Concomitantly, the hCVPC-reduced TUNEL⁺ cardiomyocytes (Figure 7C,D) and cCas-3 level (Figure 7E) in the infarct and border zones of I/R hearts were reversed to the level in the I/R group. Moreover, the NT-3-Ab treatment cancelled hCVPC-mediated enhancement in the P-ERK and suppression in the Bim level in the I/R hearts (Figure 7F).

4 | DISCUSSION

These results confirm that implantation of hCVPCs at the onset of reperfusion can improve cardiac function and reduce fibrosis in I/R hearts. These beneficial effects are at least related to the improvement of existing cardiomyocyte survival and angiogenesis in I/R hearts. Moreover, we found that hCVPCs highly secrete NT-3 and delivery of hNT-3 to I/R hearts or to sl/R AMCMs at the beginning of reperfusion mimics the beneficial effects of hCVPCs, whereas NT-3 antibody cancels the beneficial effects of hCVPCs. Furthermore, we showed that NT-3 exists in AMCMs and AMCFs, and downregulation of endogenous NT-3 in murine hearts aggravates myocardial I/R

injury, accompanied with enhanced cardiomyocyte apoptosis and reduced vessel density. Mechanistically, in addition to the enhancement of vessel density in the infarcted hearts, hCVPC-secreted NT-3 and endogenous NT-3 attenuate I/R-induced apoptosis of cardiomyocytes through the activation of ERK, thereby reducing the level of Bim, a key mitochondrial apoptosis activator, and promoting the healing of infarcted hearts. These findings reveal a previously unrecognized paracrine factor of hCVPCs and identify new roles of hCVPC-secreted endogenous protein NT-3 in cardiac protection against myocardial I/R injury. The findings also provide new insights into the cardioprotective mechanisms of NT-3 in cardiac repair.

Several novel observations have been obtained from the present study. Firstly, we demonstrated that NT-3 is abundantly secreted from hCVPCs and critically contributes to hCVPC-mediated cardiac repair following I/R injury. NT-3 is produced in neuronal cells,²⁴ cardiovascular cells,²⁵ and stem cells, such as human mesenchymal stem cells (MSCs),⁴² neural stem cells,⁴³ and hESCs.⁴⁴ The generation of NT-3 in multiple cells indicates that NT-3 serves pivotal functions in the maintenance of normal development and organ function in both physiological and pathological conditions via autocrine and paracrine mechanisms. It has been shown that NT-3 is an essential factor for mammalian great vessel and cardiac development,^{25,29} promotes angiogenesis²⁶ and cardiomyocyte hypertrophy.²⁸ Our findings are the first to identify NT-3 as an important paracrine factor in hCVPC-mediated cardioreparative effects. This is supported by the high concentration of NT-3 in hCVPC-CdM and the abolishment of cardioreparative effects of hCVPCs in I/R hearts and the protection of hCVPC-CdM in sI/R cardiomyocytes by NT-3-Ab. It has been reported that MSC transplantation-mediated improvement of functional outcome in animal models of neurological disorders is partially associated with the secretion of NT-3,⁴² indicating that NT-3 appears to contribute to the reparative effects associated with stem cell therapy. Therefore, to thoroughly dissect the secretome of hPSC-derived cardiac lineage cells and to elucidate how these factors and EVs/exosomes protect I/R hearts would be of great value for the development of new therapeutic approaches for ischemic heart disease.

Secondly, results from this study reveal the dynamic expression pattern and the role of endogenous NT-3 in I/R hearts. Although NT-3 is detected in adult rat cardiomyocytes,²⁸ the dynamic pattern of NT-3 protein levels during myocardial I/R is unknown. Our results demonstrated the existence of NT-3 protein in AMCMs and AMCFs. The NT-3 protein levels tend to decrease at the beginning of reperfusion and then upregulate in the infarct and border zones at day 3 to day 7 post-reperfusion in adult murine hearts. Similarly, upregulation of NT-3 mRNA is detected at day 3 following ischemia in murine skeletal muscle.²⁶ Moreover, the expression of nerve growth factor increases following hypoxia/reoxygenation in cultured rat neonatal cardiomyocytes.⁴⁵ These observations suggest that enhancement of NT-3 represents an endogenous protective mechanism for repairing damaged tissue. This is supported by our data showing that downregulation of endogenous NT-3 in adult murine hearts significantly deteriorates myocardial I/R injury, characterized by worsened LV

function and enhanced fibrosis formation, whereas the opposite effects are observed after injection of exogenous hNT-3 into the I/R hearts at the beginning of reperfusion followed by a 6-day continuously subcutaneous administration of hNT-3. The protective effects of exogenous delivery of NT-3 are observed in mouse models of limb ischemia²⁶ and in cerebral I/R injury.⁴⁶ Thus, NT-3 is an endogenous protective factor and might act as a novel potential agent for the treatment of ischemic heart diseases.

Thirdly, our results provide the first insight and define the underlying mechanisms of the protective function of NT-3 in cardiomyocytes subjected to I/R injury. This is supported by the following observations: (i) AMCMs express NT-3; (ii) myocardial I/R-induced apoptosis of cardiomyocytes is significantly reduced by upregulation of NT-3 with exogenous hNT-3, whereas cardiomyocyte apoptosis increases with downregulation of endogenous NT-3 with Ad-shNT-3 or neutralization of NT-3 with its neutral antibody in adult mice hearts subjected to I/R injury; and (iii) similar results are further confirmed in sI/R AMCMs. In addition, the angiogenic effects of NT-3 in I/R hearts are consistent with observations in a murine model of limb ischemia.^{25,26} Therefore, improved cardiac function and reduced fibrosis formation by implantation of hCVPCs and exogenous hNT-3 in I/R hearts are at least related to the improvement of cardiomyocyte survival and angiogenesis. As NT-3 is expressed in cardiac fibroblasts, the regulatory effect of NT-3 in fibroblasts and its contribution to fibrosis formation in I/R hearts need to be determined in the future. It has been documented that activation of prosurvival kinases (such as Akt and ERK) can achieve powerful cardioprotection when activated at the time of myocardial reperfusion.^{4,33,47} However, activation of these pathways at the time of myocardial reperfusion is not sufficient to confer cardioprotection, and additional stimulus are needed to increase the activation of these pathways to effectively protect the heart against I/R injury.^{34,48} NT-3 can activate kinase cascades such as Akt in microvascular endothelial cells of limb,²⁶ P38 in glioblastoma cells⁴⁹ or ERK in Müller cells⁵⁰ via binding to TrkC to play a fundamental role in cell survival and proliferation after ischemic injury.²⁵ Interestingly, we observed that at day 1 post-reperfusion I/R-increased phosphorylation of ERK is further enhanced by injection of exogenous hNT-3 or hCVPCs but not the phosphorylation of AKT and P38, whereas the activation of ERK and the cardioprotective effects of hNT-3 are abolished by an ERK specific inhibitor, SCH772984. Therefore, activation of the ERK signaling pathway is responsible for the NT-3-mediated cardioprotection, including the improvement of cardiomyocyte survival in I/R hearts. This is further supported by observations that enhanced Bim (a directly downstream target of activated ERK⁴⁰), in I/R hearts is significantly inhibited by hNT-3, concomitantly with decrease of cCas-3 in sI/R cardiomyocytes. However, opposite effects are observed in I/R hearts and sI/R cardiomyocytes with SCH772984 treatment. RSK is another direct downstream target of phosphorylated ERK,^{41,51} which has the opposite role to Bim in apoptosis where RSK inhibiting apoptosis but Bim initiating apoptosis.⁴⁰ As phosphorylation of RSK is not altered in I/R hearts with or without hNT-3 treatment, the ERK-Bim-caspase 3 pathway contributes to the NT-3-mediated prosurvival effects in cardiomyocytes

during the healing process of I/R hearts. Other proteins secreted from hCVPCs could be involved in the modulation of apoptosis in cardiomyocytes and angiogenesis, resulting in promoting of infarct heart healing. It is worthy further study to thoroughly identify potentially secreted-proteins from hCVPCs which contribute to cardioprotection. These findings, together with the observations of the cardiac benefits from various cell-based therapies when delivered during the early phase of I/R or MI,^{7,8,15} suggest that the paracrine effects are a critical mechanism in cell-based therapies for myocardial I/R via triggering of endogenous cardioprotective and repair programs.^{52,53} Thus, further characterization of the stem cell secretome and identification of specific paracrine factors would provide an opportunity to develop protein therapeutics that protect and repair damaged hearts.

In this study, we showed that the improvement of cardiomyocyte survival and vascularization in the infarcted hearts by hCVPCs and hNT-3 are associated with the better cardiac function and reduced fibrosis formation. This is consistent with previous reports showing that anti-apoptosis/necrosis of cardiomyocytes and/or improvement of angiogenesis can significantly reduce scar size in MI or I/R hearts.^{54,55} Because MI and I/R cause apoptosis/necrosis of cardiomyocytes and destroy capillary networks, to rebuild vascular network after MI or I/R is essential for delivering oxygen and metabolites to cardiac cells to help recovery of damaged cells and thereby links to reduce scar size.^{1,54,56-58} Thus, therapeutic approaches that improve myocyte survival and angiogenesis in infarcted hearts are beneficial for reduction of fibrosis formation.

5 | CONCLUSION

We have demonstrated that NT-3 is a novel endogenous cardioprotective factor secreted from hCVPCs and is enhanced in the I/R heart. It contributes to the delivery of hCVPC-mediated improvement of cardiac function and limitation of fibrosis formation, and the endogenous NT-3 in the hearts attenuates myocardial I/R injury too. The beneficial effects of NT-3 are the result of improvement of cardiomyocyte survival through the ERK-Bim signaling pathway and the promotion of angiogenesis in I/R hearts. The findings provide novel insights into the role and mechanisms of the neurotrophin family member in the improvement of cardiomyocyte survival in I/R hearts, the paracrine action of hCVPCs in cell therapies for the ischemic heart disease, and the value of cell products in cell-free approaches for the treatment of ischemic heart disease.

ACKNOWLEDGMENTS

This work was supported by grants from National Key R&D Program of China (2017YFA0103700 and 2016YFC1301204 to YHT), the Strategic Priority Research Program of the Chinese Academy of Sciences (No. XDA16010201 to YHT), National Natural Science Foundation of China (81520108004 and 81470422 to YHT, 81500235 to LML), and Major Program of Development Fund for Shanghai Zhangjiang National Innovation Demonstration Zone (ZJ2018-ZD-004 to YHT)

and the Science and Technology Commission of Shanghai Municipality (17431906600 to YHT). The authors thank Mr. Xiujian Yu in Shanghai Institute of Nutrition and Health for the technical support and thank WiCell Research Institute for providing the H9 hESCs.

CONFLICT OF INTEREST

The authors declared no potential conflicts of interest.

AUTHOR CONTRIBUTIONS

W.B., J.W.: conception and design, collection and assembly of data, data analysis and interpretation, manuscript writing; Y.J.: provided hCVPCs, performed part experiments of immunofluorescence staining; Q. Li: designed research, isolated some adult mice cardiomyocytes, manuscript writing; S.W.: provided hCVPC-CdM; M. L.: financial support, collection of in vitro data; Q. Liu: performed the in vitro experiments; proteome analyses of hESC-CVPC-conditional medium; F.L.: reagent ordering and other support; C.P.: manuscript revision and language editing; Y.W.: data analysis, manuscript revision; H.T.Y.: conception and design, data analysis and interpretation, manuscript writing, financial support, final approval of manuscript.

DATA AVAILABILITY STATEMENT

The data that support the findings of this study are available from the corresponding author upon reasonable request.

ORCID

Qiang Li  <https://orcid.org/0000-0002-1417-9908>

Huang-Tian Yang  <https://orcid.org/0000-0002-6297-9037>

REFERENCES

1. Prabhu SD, Frangogiannis NG. The biological basis for cardiac repair after myocardial infarction: from inflammation to fibrosis. *Circ Res*. 2016;119:91-112.
2. Ivey MJ, Kuwabara JT, Pai JT, Moore RE, Sun Z, Tallquist MD. Resident fibroblast expansion during cardiac growth and remodeling. *J Mol Cell Cardiol*. 2018;114:161-174.
3. Yellon DM, Hausenloy DJ. Myocardial reperfusion injury. *N Engl J Med*. 2007;357:1121-1135.
4. Davidson SM, Ferdinandy P, Andreadou I, et al. Multitarget strategies to reduce myocardial ischemia/reperfusion injury: Jacc review topic of the week. *J Am Coll Cardiol*. 2019;73:89-99.
5. Menasche P, Vanneau V, Hagege A, et al. Transplantation of human embryonic stem cell-derived cardiovascular progenitors for severe ischemic left ventricular dysfunction. *J Am Coll Cardiol*. 2018;71:429-438.
6. Fernandes S, Chong JJH, Paige SL, et al. Comparison of human embryonic stem cell-derived cardiomyocytes, cardiovascular progenitors, and bone marrow mononuclear cells for cardiac repair. *Stem Cell Rep*. 2015;5:753-762.
7. Zhu K, Wu Q, Ni C, et al. Lack of remuscularization following transplantation of human embryonic stem cell-derived cardiovascular progenitor cells in infarcted nonhuman primates. *Circ Res*. 2018;122:958-969.
8. Berry JL, Zhu W, Tang YL, et al. Convergences of life sciences and engineering in understanding and treating heart failure. *Circ Res*. 2019;124:161-169.
9. Polhemus DJ, Trivedi RK, Sharp TE, et al. Repeated cell transplantation and adjunct renal denervation in ischemic heart failure: exploring

- modalities for improving cell therapy efficacy. *Basic Res Cardiol.* 2019; 114:9.
10. Saha P, Sharma S, Korutla L, et al. Circulating exosomes derived from transplanted progenitor cells aid the functional recovery of ischemic myocardium. *Sci Transl Med.* 2019;11:eaau1168.
 11. Zhao L, Cheng G, Choksi K, et al. Transplantation of human umbilical cord blood-derived cellular fraction improves left ventricular function and remodeling after myocardial ischemia/reperfusion. *Circ Res.* 2019;125:759-772.
 12. Bolli R, Kahlon A. Time to end the war on cell therapy. *Eur J Heart Fail.* 2020;22:893-897.
 13. Schwach V, Gomes Fernandes M, Maas S, et al. Expandable human cardiovascular progenitors from stem cells for regenerating mouse heart after myocardial infarction. *Cardiovasc Res.* 2020;116:545-553.
 14. Gao L, Gregorich ZR, Zhu W, et al. Large cardiac muscle patches engineered from human induced-pluripotent stem cell-derived cardiac cells improve recovery from myocardial infarction in swine. *Circulation.* 2018;137:1712-1730.
 15. Wang J, Liu M, Wu Q, et al. Human embryonic stem cell-derived cardiovascular progenitors repair infarcted hearts through modulation of macrophages via activation of signal transducer and activator of transcription 6. *Antioxid Redox Signal.* 2019;31:369-386.
 16. Romagnuolo R, Masoudpour H, Porta-Sanchez A, et al. Human embryonic stem cell-derived cardiomyocytes regenerate the infarcted pig heart but induce ventricular tachyarrhythmias. *Stem Cell Rep.* 2019;12:967-981.
 17. Bargehr J, Ong LP, Colzani M, et al. Epicardial cells derived from human embryonic stem cells augment cardiomyocyte-driven heart regeneration. *Nat Biotechnol.* 2019;37:895-906.
 18. Blin G, Nury D, Stefanovic S, et al. A purified population of multipotent cardiovascular progenitors derived from primate pluripotent stem cells engrafts in postmyocardial infarcted nonhuman primates. *J Clin Invest.* 2010;120:1125-1139.
 19. Cao N, Liang H, Huang J, et al. Highly efficient induction and long-term maintenance of multipotent cardiovascular progenitors from human pluripotent stem cells under defined conditions. *Cell Res.* 2013;23:1119-1132.
 20. Cao N, Liang H, Yang HT. Generation, expansion, and differentiation of cardiovascular progenitor cells from human pluripotent stem cells. *Methods Mol Biol.* 2015;1212:113-125.
 21. Kervadec A, Bellamy V, El Harane N, et al. Cardiovascular progenitor-derived extracellular vesicles recapitulate the beneficial effects of their parent cells in the treatment of chronic heart failure. *J Heart Lung Transplant.* 2016;35:795-807.
 22. El Harane N, Kervadec A, Bellamy V, et al. Acellular therapeutic approach for heart failure: in vitro production of extracellular vesicles from human cardiovascular progenitors. *Eur Heart J.* 2018;39:1835-1847.
 23. Wu Q, Wang J, Tan WLW, et al. Extracellular vesicles from human embryonic stem cell-derived cardiovascular progenitor cells promote cardiac infarct healing through reducing cardiomyocyte death and promoting angiogenesis. *Cell Death Dis.* 2020;11:354.
 24. Scott-Solomon E, Kuruvilla R. Mechanisms of neurotrophin trafficking via trk receptors. *Mol Cell Neurosci.* 2018;91:25-33.
 25. Caporali A, Emanuelli C. Cardiovascular actions of neurotrophins. *Physiol Rev.* 2009;89:279-308.
 26. Cristofaro B, Stone OA, Caporali A, et al. Neurotrophin-3 is a novel angiogenic factor capable of therapeutic neovascularization in a mouse model of limb ischemia. *Arterioscler Thromb Vasc Biol.* 2010; 30:1143-1150.
 27. Lu B, Pang PT, Woo NH. The yin and yang of neurotrophin action. *Nat Rev Neurosci.* 2005;6:603-614.
 28. Kawaguchi-Manabe H, Ieda M, Kimura K, et al. A novel cardiac hypertrophic factor, neurotrophin-3, is paradoxically downregulated in cardiac hypertrophy. *Life Sci.* 2007;81:385-392.
 29. Donovan MJ, Hahn R, Tessarollo L, Hempstead BL. Identification of an essential nonneuronal function of neurotrophin 3 in mammalian cardiac development. *Nat Genet.* 1996;14:210-213.
 30. Gu S, Tan J, Li Q, et al. Downregulation of laptm4b contributes to the impairment of the autophagic flux via unopposed activation of mtorc1 signaling during myocardial ischemia/reperfusion injury. *Circ Res.* 2020;127:e148-e165.
 31. Tokunaga M, Liu ML, Nagai T, et al. Implantation of cardiac progenitor cells using self-assembling peptide improves cardiac function after myocardial infarction. *J Mol Cell Cardiol.* 2010;49:972-983.
 32. Ichihara Y, Kaneko M, Yamahara K, et al. Self-assembling peptide hydrogel enables instant epicardial coating of the heart with mesenchymal stromal cells for the treatment of heart failure. *Biomaterials.* 2018;154:12-23.
 33. Chen Y, Liu J, Zheng Y, et al. Uncoupling protein 3 mediates h(2)o (2) preconditioning-afforded cardioprotection through the inhibition of mptp opening. *Cardiovasc Res.* 2015;105:192-202.
 34. Zheng Y, Gu S, Li X, et al. Berbamine postconditioning protects the heart from ischemia/reperfusion injury through modulation of autophagy. *Cell Death Dis.* 2017;8:e2577.
 35. Li J, Yousefi K, Ding W, Singh J, Shehadeh LA. Osteopontin rna aptamer can prevent and reverse pressure overload-induced heart failure. *Cardiovasc Res.* 2017;113:633-643.
 36. Wang ZH, Chen YX, Zhang CM, et al. Intermittent hypobaric hypoxia improves postischemic recovery of myocardial contractile function via redox signaling during early reperfusion. *Am J Physiol Heart Circ Physiol.* 2011;301:H1695-H1705.
 37. Xie M, Kong Y, Tan W, et al. Histone deacetylase inhibition blunts ischemia/reperfusion injury by inducing cardiomyocyte autophagy. *Circulation.* 2014;129:1139-1151.
 38. Garcia-Prieto J, Garcia-Ruiz JM, Sanz-Rosa D, et al. Beta3 adrenergic receptor selective stimulation during ischemia/reperfusion improves cardiac function in translational models through inhibition of mptp opening in cardiomyocytes. *Basic Res Cardiol.* 2014;109:422.
 39. Wu L, Tan JL, Wang ZH, et al. Ros generated during early reperfusion contribute to intermittent hypobaric hypoxia-afforded cardioprotection against postischemia-induced Ca(2+) overload and contractile dysfunction via the jak2/stat3 pathway. *J Mol Cell Cardiol.* 2015;81:150-161.
 40. Mebratu Y, Tesfaigzi Y. How erk1/2 activation controls cell proliferation and cell death: is subcellular localization the answer? *Cell Cycle.* 2009;8:1168-1175.
 41. Lim W, Yang C, Bazer FW, Song G. Chrysophanol induces apoptosis of choriocarcinoma through regulation of ros and the akt and erk1/2 pathways. *J Cell Physiol.* 2017;232:331-339.
 42. Volkman R, Offen D. Concise review: mesenchymal stem cells in neurodegenerative diseases. *STEM CELLS.* 2017;35:1867-1880.
 43. Gu YL, Yin LW, Zhang Z, et al. Neurotrophin expression in neural stem cells grafted acutely to transected spinal cord of adult rats linked to functional improvement. *Cell Mol Neurobiol.* 2012;32: 1089-1097.
 44. Pyle AD, Lock LF, Donovan PJ. Neurotrophins mediate human embryonic stem cell survival. *Nat Biotechnol.* 2006;24:344-350.
 45. Caporali A, Sala-Newby GB, Meloni M, et al. Identification of the prosurvival activity of nerve growth factor on cardiac myocytes. *Cell Death Differ.* 2008;15:299-311.
 46. Duricki DA, Hutson TH, Kathe C, et al. Delayed intramuscular human neurotrophin-3 improves recovery in adult and elderly rats after stroke. *Brain.* 2016;139:259-275.
 47. Hausenloy DJ, Yellon DM. Reperfusion injury salvage kinase signaling: taking a risk for cardioprotection. *Heart Fail Rev.* 2007;12: 217-234.
 48. Hausenloy DJ, Barrabes JA, Botker HE, et al. Ischaemic conditioning and targeting reperfusion injury: a 30 year voyage of discovery. *Basic Res Cardiol.* 2016;111:70.



49. Jawhari S, Besette B, Hombourger S, et al. Autophagy and trkc/nt-3 signaling joined forces boost the hypoxic glioblastoma cell survival. *Carcinogenesis*. 2017;38:592-603.
50. Li N, Gao S, Wang J, Zhu Y, Shen X. Anti-apoptotic effect of interleukin-17 in a mouse model of oxygen-induced retinopathy. *Exp Eye Res*. 2019;187:107743.
51. Romeo Y, Zhang X, Roux PP. Regulation and function of the rsk family of protein kinases. *Biochem J*. 2012;441:553-569.
52. Menasche P. Cell therapy trials for heart regeneration-lessons learned and future directions. *Nat Rev Cardiol*. 2018;15:659-671.
53. Li Q, Wang J, Wu Q, Cao N, Yang HT. Perspective on human pluripotent stem cell-derived cardiomyocytes in heart disease modeling and repair. *STEM CELLS TRANSLATIONAL MEDICINE*. 2020;9:1121-1128.
54. Zhang J, Ding L, Zhao Y, et al. Collagen-targeting vascular endothelial growth factor improves cardiac performance after myocardial infarction. *Circulation*. 2009;119:1776-1784.
55. Liang J, Huang W, Jiang L, Paul C, Li X, Wang Y. Concise review: reduction of adverse cardiac scarring facilitates pluripotent stem cell-based therapy for myocardial infarction. *STEM CELLS*. 2019;37:844-854.
56. Broughton KM, Wang BJ, Firouzi F, et al. Mechanisms of cardiac repair and regeneration. *Circ Res*. 2018;122:1151-1163.
57. Ma Y, Iyer RP, Jung M, Czubyrt MP, Lindsey ML. Cardiac fibroblast activation post-myocardial infarction: current knowledge gaps. *Trends Pharmacol Sci*. 2017;38:448-458.
58. Liang J, Huang W, Cai W, et al. Inhibition of microrna-495 enhances therapeutic angiogenesis of human induced pluripotent stem cells. *STEM CELLS*. 2017;35:337-350.

SUPPORTING INFORMATION

Additional supporting information may be found online in the Supporting Information section at the end of this article.

How to cite this article: Bi W, Wang J, Jiang Y, et al. Neurotrophin-3 contributes to benefits of human embryonic stem cell-derived cardiovascular progenitor cells against reperfused myocardial infarction. *STEM CELLS Transl Med*. 2021;10:756–772. <https://doi.org/10.1002/sctm.20-0456>